Talanta 84 (2011) 1099–1106

Contents lists available at ScienceDirect

Talanta

journal homepage: www.elsevier.com/locate/talanta

A facile light-emitting-diode induced fluorescence detector coupled to an integrated microfluidic device for microchip electrophoresis

Fan Yang, Xin-chun Li, Wen Zhang, Jian-bin Pan, Zuan-guang Chen*

School of Pharmaceutical Sciences, Sun Yat-sen University, Guangzhou, Guangdong 510006, PR China

ARTICLE INFO

Article history:
Received 18 January 2011
Received in revised form 3 March 2011
Accepted 8 March 2011
Available online 16 March 2011

Keywords:
Microchip electrophoresis
Fluorescence detection
Light emitting diode
Miniaturization
Penicillamine

ABSTRACT

In this paper, a compact and inexpensive light emitting diode induced fluorescence (LED-IF) detector with simplified optical configuration was developed and assembled in an integrated microfluidic device for microscale electrophoresis. The facile detector mainly consisted of an LED, a focusing pinhole, an emission filter and a photodiode, and was encapsulated in the upper layer of an aluminum alloy device with two layers. At the bottom layer, integrated circuit (IC) was assembled to manipulate the voltage for sample injection and separation, LED emission and signal amplifying. A high-power LED with fan-shaped heat sink was used as excitation source. The excitation light was focused by a 1.1 mm diameter pinhole fabricated in a thin piece of silver foil, and the obtained sensitivity was about 3 times as high as that using electrode plate. Other important parameters including LED driven current, fluorescence collection angle and detection distance have also been investigated. Under optimal conditions, considerable high-response of 0.09 fmol and 0.18 fmol mass detection limits at 0.37 nL injection volume for sodium fluorescein (SF) and FITC was achieved, respectively. This device has been successfully employed to separate penicillamine (PA) enantiomers. Due to such significant features as low-cost, integration, miniaturization, and ease of commercialization, the presented microfluidic device may hold great promise for clinical diagnostics and bioanalytical applications.

© 2011 Elsevier B.V. All rights reserved.

1. Introduction

To realize the miniaturization, low-cost, and extended application for microfluidic device, the small size, simple and sensitive detectors are essential and play an ever-increasingly important role. Up to now, except for laser-induced fluorescence (LIF) [1], many other detecting schemes including ultraviolet (UV) [2], mass spectrometry (MS) [3], chemiluminescence (CL) [4], electrochemiluminescence (ECL) [5], electrochemistry (EC) [6], nuclear magnetic resonance (NMR) [7] and electromagnetic conductivity (EMC) [8,9], as well as dual detectors [10,11], have been designed and integrated with microfluidic system. LIF detection as one of the most sensitive detectors has been widely employed in biomedical analysis, with a sensitivity even up to single molecule level [12]. However, the disadvantages of laser such as comparatively expensive, bulky, high power consumption, limited spectral range and relatively short life span have constrained its further integration with microdevice. Although the relatively small and inexpensive laser diodes have improved lasers to some extent, it still suffers from limited spectral range and high power consumption [13]. Therefore, other effective alternatives should be available for excitation light source.

Recently, great attention has been paid to the light-emitting diodes (LEDs) as alternate light sources for microscale fluorescence detection, owing to low cost, small size, wide wavelength range, low-power consumption and long lifetime ($>5 \times 10^4$ h) [14]. Currently, LED including organic (OLED) and inorganic LED, have integrated with different microsystems. Yao and co-workers develop a microfluidic device assembly with a green OLED for proteins analysis, 1.4 fmol and 35 fmol mass detection limits at 0.7 nL injection volume for Alexa and Rhodamine dye have been obtained, respectively [15]. In addition, Edel et al. present a thin-film polymer light emitting diode (pLED) as an integrated excitation source in microchip for fluorescein and 5-carboxyfluorescein detection, with a mass detection limit of 50 fmol achieved [16]. Following that, they design a disposable diagnostic microchip based on a thin-film OLED to determine microalbuminuria [17]. Despite the wide use of OLED in microchip, its high cost and immature commercialization limit its prevalence. In contrast, inorganic LEDs, namely conventional LED, are commercially available with low-cost, currently. Chabinyc and co-workers have developed a prototype microdevice integrated with a LED-IF detector, which uses a blue LED as light source and directs the excitation light by a 100 μm core diameter multimode optical fiber (OF) encapsulated in PDMS [18].

* Corresponding author. Tel.: +86 20 3994 3044; fax: +86 20 3994 3071.
E-mail address: chenzg@mail.sysu.edu.cn (Z.-g. Chen).

0039-9140/$ – see front matter © 2011 Elsevier B.V. All rights reserved.
doi:10.1016/j.talanta.2011.03.020

Moreover, Liu et al. describe a PDMS sandwich microchip equipped with OF by completely contacting with the separation channel to couple excitation light from LED for fluorescence detection [19]. Except for integrating with PDMS-based microchip, LED has also been assembled in glass chip. Du et al. present a high-throughput glass chip-based flow-injection analysis (FIA) system with gravity-driven flows and use a LED light source for liquid-core waveguide (LCW) spectrometric detection [20]. In our previous work, a dual detector consisted of a LED-IF detector and a contactless conductivity detector has been developed for common point detection in microchip [10]. It is believed that the free-modification glass microchip equipped with LED-IF detection can facilitate complex sample assay.

Besides light source, optical arrangement of LIF detection is another key factor for detection sensitivity and device fabrication. Since LED, first, used as light source in CE [21], many groups have so far developed varied optical setups including orthogonal [22], confocal [23] and in-column excitation mode [24] for capillary electrophoresis. Due to the planar chip-based structure, it is not well-suited for conventional orthogonal or confocal structures. Even though the orthogonality can effectively prevent the excitation from straightforward irradiating on the photodetector, it is not compatible with microchip ascribed to unpolished sidewall surfaces and complicated microchannel layout [1]. In addition, particular requirements for dichroic mirror position and lens confocal distance in a typical confocal design limit its wide application in microsystem. Thus, parallel and intersectant (defined by angle between excitation and emission path) optical arrangements have been adopted to realize the improvement of sensitivity and the miniaturization of microdevice. As for the former design, a collinear or parallel geometry would be implemented by placing the excitation source and the photodetector above or below the surface of microchip. Therefore, a high quality filter or filter group should be applied in front of detector to effectively distinguish the excitation and emission light since the light source would directly impinge upon the detector [25]. Some groups have employed this optical configuration. Yao et al. insert a 300 μm-thick TiO_2/SiO_2 interference filter between the light source and microchannel in a parallel setup to eliminate unwanted excitation light [15]. More interestingly, Hofmann and co-workers fabricate the monolithically integrated optical long-pass filters by incorporating dye molecules directly into the microchip substrate, PDMS, to block the excitation light and pass only the longer wavelength emission signal [25]. Obviously, this optical arrangement requires expensive filters and OLEDs, which need time-consuming and labor intensive preparation though the detector is highly miniaturized. Instead, intersectant setup has also been used in the microchip system. Schrum and co-workers have developed a glass microchip flow cytometry integrated with laser light scattering and fluorescence coincidence measurements with a 45° incident angle for excitation [26]. Unfortunately, the use of coincidence measurements masks the advantages of this optical design for further application in glass microscale system.

Usually, a typical LED-IF detector was composed of light sources, microlenses, filters, mirrors, optical fibers (OFs), gratings and photodetectors. However, so many optical elements, undoubtedly, provide complicated fabrication, high-cost and large size for detector. In addition, the use of OF adds additional techniques and many other disadvantages, such as relatively large size, time consuming modification to the end of OF [27] and irreversible OF positioning [28], to detector fabrication.

In this paper, a novel free-OF and low-cost LED-IF detector with simplified optical arrangement was fabricated and assembled in an integrated microdevice for microchip electrophoresis. We used a high-power LED with heat-eliminating plate as excitation source and a small size of 1.1 mm diameter pinhole drilled in a thin piece of silver foil was applied to focus excitation beam. Such a simple design could meet the requirements of more microchip compared to previous dual detector. Furthermore, different functionalized integrated circuit (IC), such as sample separation high voltage, sample injection voltage, LED driven and signal amplifier electric circuit, were incorporated into the bottom layer of a newly designed small metallic device. The effects of LED driven current, pinhole size, fluorescence collection angle, photodiode position and glass microchip thickness on detection sensitivity have been investigated. Under optimized conditions, the performance of our proposed microfluidic device with present optical setup was evaluated by detecting sodium fluorescein (SF) and FITC, respectively. Using this device, the PA enantiomers were separated.

2. Experimental

2.1. Chemicals

Fluorescein isothiocyanate (FITC), sodium fluorescein (SF) and β-CD were purchased from Sinopharm Group Chemical Reagent Co. Ltd. (Shanghai, China). Sodium dodecyl sulfate (SDS) were obtained from Shanghai Sangon Biological Engineering Technology & Services Co. Ltd. (Shanghai, China). D and D/L penicillamine (PA) were purchased from Shanghai Crystal Pure Reagent Co. Ltd. (Shanghai, China). Other analytical-grade reagents were obtained from Guangzhou Chemical Reagent Co. (Guangzhou, China). The labeling FITC solution (10 mmol L^{-1}) was prepared in acetone with 1% pyridine and kept in the dark at 4 °C. The running buffer solution of 100 mmol L^{-1} borate was prepared and diluted to suitable concentration prior to use. Sodium fluorescein, D- and D/L PA were prepared with water to a concentration of 10 mmol L^{-1} as stock solutions, respectively. Milli-Q water (Millipore, Bedford, MA, USA) was used throughout the work. All solutions were filtered through a 0.22 μm membrane filter before being loaded to the inlet and outlet reservoirs.

2.2. Apparatus and equipment

An integrated microfluidic device with facile optically arranged light emitting diode induced fluorescence detection was established and shown in Fig. 1(A). This homemade device was composed of two layers, the upper and bottom layer. Four turnbuttons on the bottom layer were used for the regulation of LED driven current, high voltage (HV), signal amplifying and baseline back to zero level, respectively. A schematic diagram of LED-IF detection system assembled in the upper layer was demonstrated in Fig. 1(B). A high brightness (HB) blue LED (SFHU10TB5HBN-L5, Shifeng Optic and Electronics Ltd., Shenzhen, China) with a fan-shaped heat sink was used as excitation source and its driving current was varied by a tunable power supply. A plastic plate with the same height as the LED was applied to make it horizontally attached to the device surface. Along the positioned LED center, three obvious marks were easily fabricated to facilitate the alignment between the pinhole center and LED surface center. The scattered excitation light emitted from LED was focused directly by a focusing pinhole drilled on a 0.5 mm-thick electrode plate, which was then replaced by the thinner materials-silver foil with several tens of micrometers in thickness. Alignment of the microchip detection point was achieved by adjusting the buffer reservoir and buffer waste reservoir positions. The focused excitation passed through the pinhole and penetrated microchip cover plate to irradiate the analyte to produce fluorescence, which then transmitted through a long pass filter (LP 510 nm, Huibo, Shenyang, China) prior to impinging upon the photodiode (Qingyue, Shanghai, China). An integrated module consisted of emission filter and photodiode was constructed

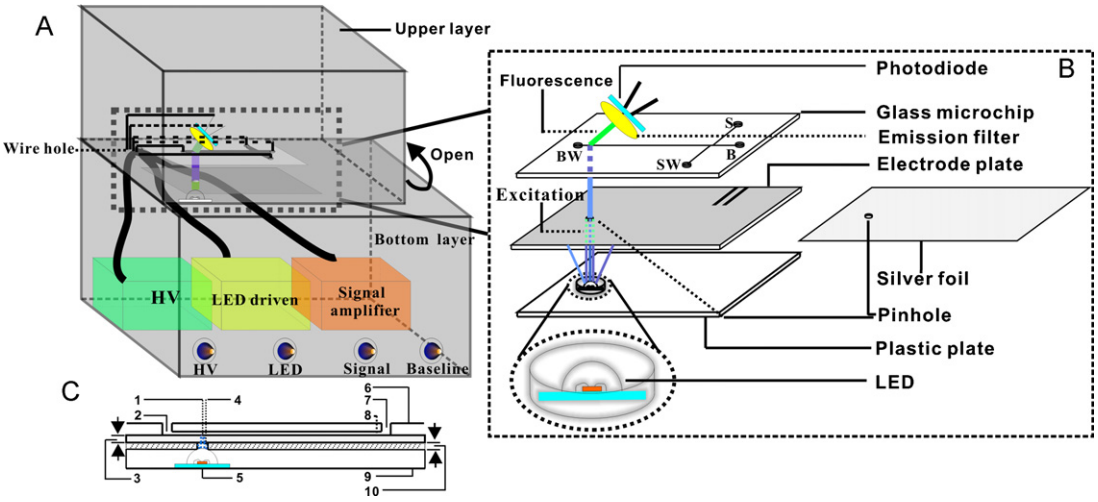

Fig. 1. The schematic of a microfluidic device integrated with LED-IF detection system. (A) Schematic diagram of the integrated microfluidic device (20 cm × 12 cm × 14 cm, $L \times W \times H$) containing two layers, the upper layer for encapsulation of the optical architecture and microchip; functionalized integrated circuit assembled in the bottom layer. (B) Detailed configuration of LED-IF detector. (C) Side view of the structure for fluorescence generation: 1, excitation; 2, outlet; 3, 1.14 mm-thick cover plate; 4, 1.10 mm-diameter pinhole; 5, LED; 6, glass substrate; 7, inlet; 8, microchannel; 9, plastic plate; 10, 1.00 mm-thick electrode plate (or silver foil).

for the convenience of its free mobility along the microchip separation channel. The module mobility range was controlled by a homemade adjustable *x*–*y* translation stage. In addition, the entire optical system was housed in a dark room, namely, the upper layer. The side view structure of fluorescence generation was presented in Fig. 1(C).

2.3. Light source

The high-power blue LED source has a peak wavelength of 470 nm with 30 nm spectral bandwidth and delivers a nominal maximum optical output power of 1 W at operating voltage and current of 3.6 V and 350 mA, respectively, at an operating temperature of 25 °C. A typical structure of the LED was shown in Fig. 2(A). This LED was integrated with a 20 mm diameter aluminum heat sink to accelerate thermal dissipation. InGaN was used as the chip material to produce high brightness blue emission. A layer of colorless transparent silicon glue was employed to prevent the chip material from environmental damage. The outermost layer of this LED was epoxy lens used as package materials to focus and collimate the light source emission, but it was removed as assembling the detector (Fig. 2(B)). In the detector fabrication, the LED source was soldered onto the metallic surface of the device bottom layer, which provided sufficient cooling for the LED at high operating current.

2.4. Microchip fabrication

In this experiment, standard photolithography, wet chemical etching, low-temperature pre-bonding and high-temperature permanent bonding techniques were used to fabricate the glass microchip [29]. Briefly, the channel pattern on a photomask was designed and transferred onto a 1.7 mm-thick, 31.6 mm × 63.2 mm glass wafer pre-coated with chromium and positive photoresist layers (Shaoguang Microelectronics Co., Changsha, China). After exposure to UV, the exposed photoresist was removed by 0.7% NaOH solution, followed by a chromium remove procedure. Subsequently, the exposed microchannel layout was etched in 1 mol L^{-1} HF + 1 mol L^{-1} NaF, with an average etch rate of 2.0 μm/min at 50 °C [29]. The etched substrate was drilled and then aligned with a cover plate for bonding at 580 °C. Another glass chip with a different cover plate, 1.1 mm-thick microscope slide, was fabricated in the same manner mentioned above. The final microchip had a double-T microchannel which was 25 μm deep and 85 μm wide (at half depth) with a 0.3 nL sample injection volume.

2.5. Precolumn derivatization

Standard D-PA solution (100 μL) and D/L PA solution (100 μL) were transferred, respectively, into a 1.5 mL polyethylene centrifuge tube containing 120 μL of 10 mmol L^{-1} FITC solution .Then the FITC solution and the target solutions were mixed and reacted over night (12 h) at 25 °C as stock solutions. Then the derivatization solutions were stored in the dark at 4 °C before use.

2.6. Chip-based CE procedure

Before use, the double-T microchannels in the CE chip were preconditioned by rinsing with 1 mol L^{-1} HNO_3 for 30 min. Between two consecutive injections, the microchannels were sequentially flushed with 0.1 mol L^{-1} NaOH, water and 10 mmol L^{-1} borate buffer, each for 5 min. The reservoir buffer, buffer waste and sample waste were filled with 30 μL electrophoretic running buffer solutions, respectively, and sample reservoir was filled with 30 μL sample solution. Four platinum (Pt) electrodes were inserted into the corresponding reservoirs for sample injection and separation. Then the detector and chip were shielded by the homemade upper layer device. In the sample loading procedure, 500 V was applied between the sample reservoir and the sample waste reservoir while other reservoirs were floated. Following an initial 15 s sample injection to ensure the intersectional channel filled with sample, the subsequent sample injection time of 10 s was enough to meet filling requirement. Then, the separation occurred by applying a potential of 2000 V to buffer reservoir and buffer waste reservoir was grounded, while other reservoirs were maintained at zero potential.

3. Results and discussion

3.1. Design of the LED-IF detection system

In this work, our major aim is to design a low-cost, easily fabricated and facile optical arrangement for fluorescence detection in microfluidic system. To that end, we constructed an inexpensive

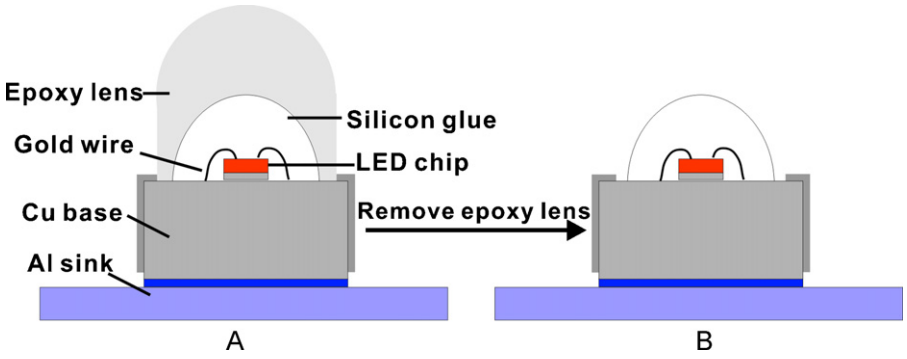

Fig. 2. (A) Schematic diagram of typical structure of a fan-shaped LED (side view). (B) The epoxy lens-removed LED (side view).

LED induced fluorescence detector including a high-power LED, an excitation focusing pinhole, a cut-off filter and a photodiode, which not only provided a competitive low cost comparable to Fang's design [22], but also demonstrated a special optical configuration compared to conventional fluorescence detection mode either used a LED or a laser as excitation source. Whatever optical structure, the most significant responsibility was to improve the detection performance as sensitive as possible.

Consequently, there are two problems dealing with signal-to-noise ratio or sensitivity to be addressed. The first question involves fluorescence signal, a key factor to obtain high sensitivity. However, the fluorescence intensity was influenced by many factors, such as excitation light intensity, wavelength match between the analyte absorption maximum and light source emission maximum, the sample characters comprising extinction coefficient and fluorescence quantum yield, and others. From Fig. 1(B), we observed that the excitation light intensity was significantly affected by the distance between the light source produced position and the microchannel for a selected LED. Thus, in most LED-IF detection already reported, optical fiber (OF) has been widely used in varied detection modes including orthogonal [22], collinear [23] and in-column fiber-optical LED-IF detector [30,31]. Although the high light conductance of OF has contributed to the improvement of its focusing capabilities, the relatively low coupling efficiency of the interface between light path may lead to excessive energy dissipation; for another, OF transmitted the excitation to the separation microchannel with rough or uneven surface, which may result in more intensive scattering at detection point, both would prompt the sensitivity deterioration. Therefore, to circumvent the problems from OF, we initially used a thin electrode plate, approximately 0.5 mm in thickness [10], to reduce the optical path. To further shorten the optical path length, we detached the epoxy lens from the LED (Fig. 2(B)) and fabricated a thin glass chip using a 1.1 mm thick microscope slide as cover plate. As shown in Table 1, the sensitivity was clearly improved compared to initial design. In addition, a piece of silver foil with several tens of micrometers was implemented to further diminish the optical span, and the sensitivity was improved nearly 3 times (Table 1). It also could be seen from the table that there was no evident enhancement in the background signal level – another significant factor for fluorescence detection, which was mainly attributed to that a cut-off filter with 510 nm wavelength could effectively eliminate the major part of noise including transmitting light penetrated through glass microchip, scattering and reflectance. Actually, the inside surface of the upper layer in this device was decorated with black paper to absorb the reflectance, refracted and strayed light for lowering the noise. Apart from the establishment of optical arrangement in the upper layer, we designed the functionalized integrated circuit responsible for LED driven, sample injection and separation, and signal acquisition, and assembled them in the bottom layer of the device (Fig. 1(A)). The entire sample analysis procedures could be accomplished in this integrated and compact system.

Table 1
The comparison of sensitivity using thin cover plate and silver foil (as pinhole materials).

	Signal[a] (mV)	Noise (mV)	S/N
Electrode plate + thick glass cover (1.7 mm)	4.18	0.09	46.44
Electrode plate + thin glass cover (1.1 mm)	4.95	0.09	55.00
Silver foil + thin glass cover (1.1 mm)	15.78	0.10	157.80

[a] Sample: 20 μmol L^{-1} sodium fluorescein; operation conditions: injection for 20 s at 0.5 kV; separation voltage, 2.0 kV; running buffer, 10 mmol L^{-1} $Na_2B_4O_7$, pH 9.2.

3.2. Optimization of the detector

3.2.1. Choice of LED, spectral filter and photodiode

The LED was characterized by low power consumption, low cost, high stability, small size, broad selective wavelengths and commercial availability, which made it a charming light source for fluorescence exciting. But its high excitation efficiency was limited by perfect match between the LED emission spectrum and the maximal excitation wavelength of the fluorescent analyte. In this experiment, both FITC (ex_{max} = 490 nm, em_{max} = 523 nm) and FS (ex_{max} = 470 nm, em_{max} = 512 nm) were applied to evaluate the system due to their high fluorescence quantum yield, reasonable extinction coefficient and cost advantage. Therefore, we used a high-power blue LED, which centered on 470 nm with a full wave at half maximum (FWHM) of 30 nm and was integrated with a fan-shaped aluminum heat sink (Fig. 2.), as excitation source in our detection system. The choice was also because of the broad availability and ease for this inexpensive LED in spite of the insufficient wavelength mismatch that occurred between the LED and FITC.

In this detector, as emitted from the LED, the excitation light would pass directly through an exquisite pinhole without an excitation filter prior to impinging on the microchannel. As a result, the scattered LED light formed the bulk of background noise. Therefore, in order to reduce or eliminate the background signal, a cut-off emission filter with 510 nm wavelength was presented before fluorescence irradiating the photodiode, and also the scattered emission of this LED was intercepted in front of the emission filter. Another advantage for this yellow filter was that the transmissivity of the emitted fluorescence wavelengths above 510 nm was 50%, which was beneficial for fluorescence collection. In addition, the Stokes' shift of both the SF and FITC was no more than 40 nm at wavelength very well suited for commercially available cut-off filters. Although the spectral filtering set consisting of excitation and emission filters in an optimized crosstalk could obtain lower background signal compared to the use of long-pass filters alone [32], it would make the optical arrangement more complex and lead to a larger size.

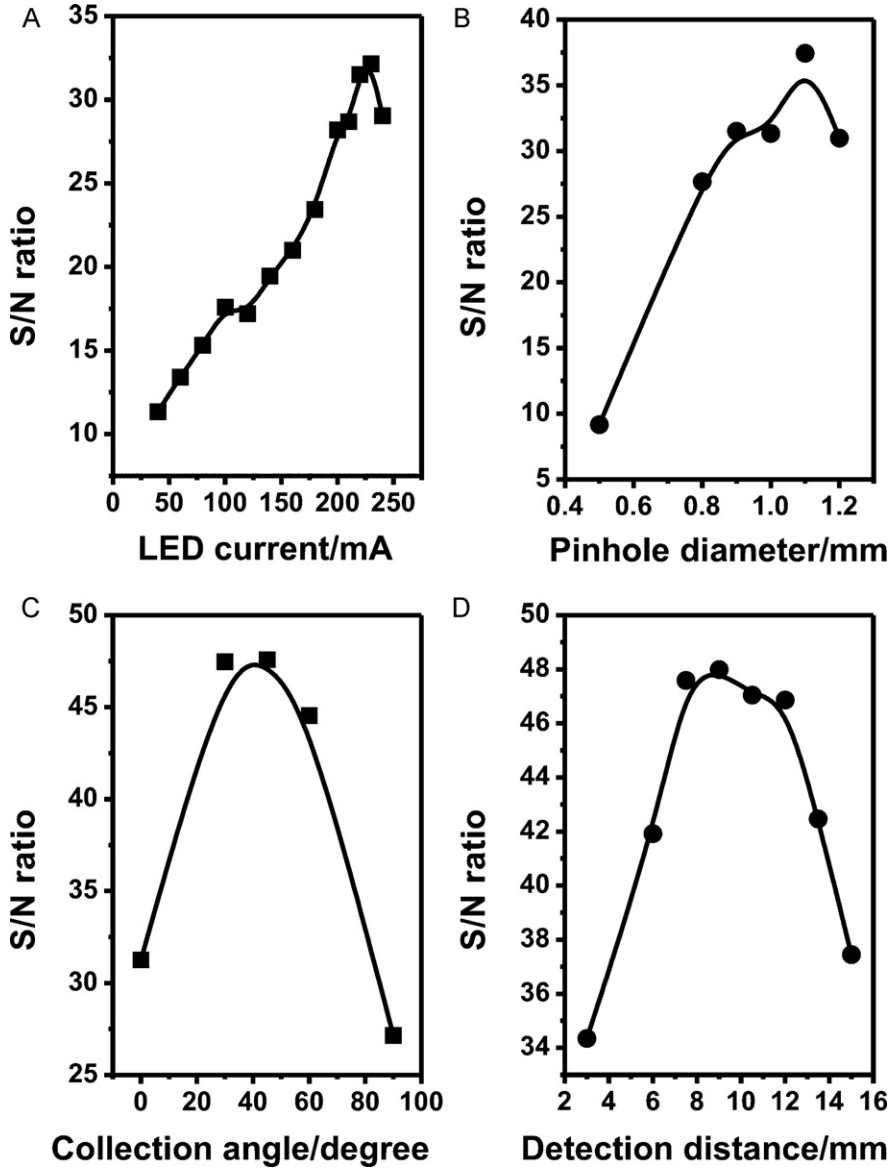

Fig. 3. Effects on LED-IF detection system. (A) The effect of driven current of LED on S/N ratio. (B) The effect of focusing pinhole diameter on S/N ratio. (C) The effect of fluorescence collection angle between the chip plane and filter-photodiode module on S/N ratio. (D) The effect of horizontal distance between focusing pinhole and filter-photodiode module on S/N ratio. Sample: 20 μmol L^{-1} sodium fluorescein; operation conditions: injection for 10 s at 0.5 kV; separation voltage, 2.0 kV; running buffer, 10 mmol L^{-1} $Na_2B_4O_7$, pH 9.2.

Under such filtering conditions, a square photodiode was used to collect the filtered fluorescence and convert them into electrical signals. This special optical cell had a size of only 12 mm × 12 mm × 2 mm ($L \times W \times H$), as compared to traditional PMT. Furthermore, the flat component was easily sandwiched between the colored filter and a thin plastic plate as an integrated element and then was connected to signal amplifier circuit. In this experiment, the photodiode response sensitivity was higher than 80% in the current fluorescence range [10], which met the experimental requirements.

3.2.2. Effect of driven current of LED

Theoretically, there has been a positive correlation between LED operating current and emission light intensity. The higher current was applied to LED, the stronger fluorescence signal was obtained. However, the maximum driven current of this LED was defined as 350 mA. In this device, a novel working circuit for LED was designed to avoid the constraints from previous FD-CCD dual detection system with a current range from 0 to 150 mA [10]. A wide driven current range from 0 to 250 mA was set in this new LED circuit to screen the optimal current. It was noted that varying working current of LED had a great impact on its performance and the result was consistent with the data obtained in previous experiment [10]. Basically, the constant increase of fluorescence signal (Fig. 3(A)) was caused by the continuous enhancement of driven current for the LED. Strangely, we observed that the device showed fast increasing of current when applied driven current was beyond 230 mA, and ultimately went beyond the current range after 1 h more or less. It was assumed that high current led to unpredicted heat production, which could affect LED performance. The reasons may be attributed to the decreasing ability of thermal management of LED packaging materials. As shown in (1) from reference [33], where R_{th} is thermal resistance, which is decided by junction temperature, ambient temperature and input thermal power:

$$R_{th} = \frac{T_j - T_0}{Q} = \sum_i^n R_{th,i} \quad (1)$$

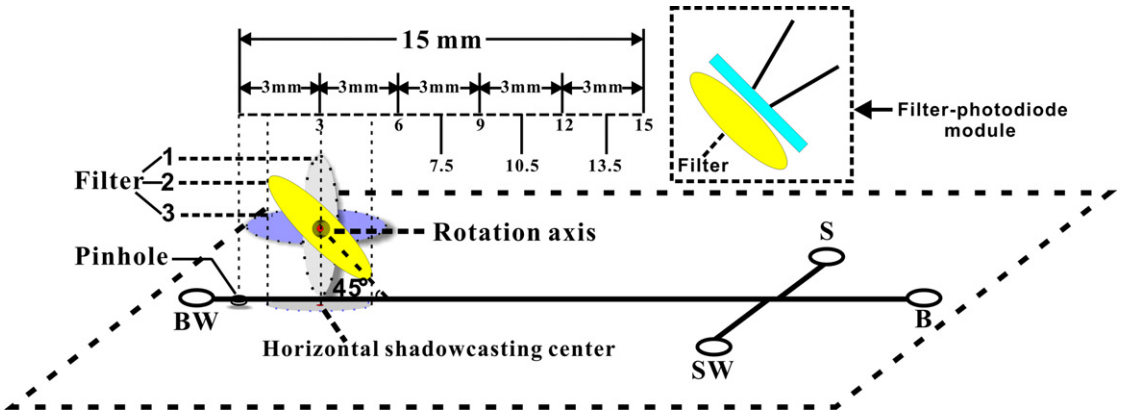

Fig. 4. Schematic diagram of fluorescence collection angle and detection distance. The filter 1, 2 and 3 are referred to three different positions with angle of 90°, 45° and 0°, respectively, between the filter-photodiode module and microchip plane. The detection distance is referred to the distance between the excitation focusing pinhole and the module horizontal shadowcasting center which coincides with microchip separation channel.

where Q is the input thermal power. T_j and T_0 are the highest junction temperature in the high bright LED and surrounding temperature, respectively. R_{th} can be referred to the assembly of thermal resistance of different packaging materials in the heat conduction path. The higher thermal resistance would result in the wider temperature gap between thermal resource and its surroundings. Consequently, the generated higher thermal stress would impair the LED packaging materials to deformation or crack, which would change the electrical resistance of LED chip. Furthermore, sequential analysis and frequent switch on driven current also contributed to the result. In fact, the intermission between each assay, could be an effective refreshment to the heated LED with a heat sink. Finally, 220 mA was chosen as the optimal driven current for the fan-shaped LED in the next experiment, and high detection sensitivity and consecutive sample manipulation were obtained without sacrificing the LED life.

3.2.3. Effect of pinhole size

The pinhole size affected both the signal and the background noise level in the measurements. During optimization of the pinhole, six pieces of electrode plate with about 0.5 mm, 0.8 mm, 0.9 mm, 1.0 mm, 1.1 mm and 1.2 mm diameter pinholes were prepared and inserted between light source and microchip for focusing the excitation light spot on chip. The larger diameter of the pinhole was used, the stronger noise level was produced and the higher fluorescence signal was obtained, but the optimal signal to noise (S/N) ratio was achieved when focusing pinhole size was set at 1.1 mm, as illustrated in the (Fig. 3(B)). Due to large divergence for emitting light originated from LED, a wider pinhole could release denser excitation to irradiate the target area on microchip. Accordingly, fluorescence signal and background noise both would be stronger. However, owing to the constant microchannel size and luminescent unit size of LED in this experiment, the excessive light pass would not lead to a higher sensitivity. Therefore, 1.1 mm diameter of pinhole was ultimately used in this system.

3.2.4. Effect of fluorescence collection angle

In this work, studies had been made on the fluorescence collection angle (defined as the angle between the chip plane and the filter plane with horizontal shadowcasting center coincided with separation channel (Fig. 4)) due to the intensive scattered light which dominated the bulk of background noise. Based on the previous work [10], we selected a series of angles, such as filter plane (filter 1) perpendicular to the chip plane with direct touch, to obtain sensitivity as high as possible and facilitate the different angles based on rotation axis (Fig. 4). The Fig. 3(C) showed that the optimal signal-to-noise ratio occurred at both 30° and 45° collection angles. But 45° fluorescence collection angle was selected instead of 30°, not only for the slightly higher sensitivity, but also for the convenience for inserting platinum (Pt) electrodes into the inlets and outlets as well as the ease of microchannel washing. It was noted that this 45° was different from the collection angle in the orthogonal structure, which used a special design and modification for microchannel and sidewall surface to improve the detection sensitivity [1].

3.2.5. Effect of detection distance

In the current LED-IF detection system, a 15 mm-long path along separation channel was identified as mobility zone for the integrated module by combining the emission filter with the flat photodiode (Fig. 4), due to operation convenience and the uniform spatial emitting property of the excited fluorescence. The effects of varied distance (from 0 to 15 mm) on the fluorescence detection sensitivity were studied. The distance was evenly divided into five parts by 3 mm, individually, and the corresponding results in Fig. 3(D) showed that the signal/background noise ratios obtained at 9.0 mm and 12.0 mm were almost identical. Therefore, to further ensure the optimal detection position, additional distance of 7.5 mm, 10.5 mm, 13.5 mm were also incorporated to optimize the results and the highest sensitivity occurred at 9.0 mm. Thus, the detection distance was finally selected at 9.0 mm, which was used in the following experiment.

3.3. Performance of the LED-IF detection system

The performance of the present LED-IF detection system was demonstrated by the analysis of sodium fluorescein (SF), FITC and D-PA (Table 2). Under the optimized condition, the

Table 2
Performance of the present LED-IF detector.

Analytes	LOD (μmol L^{-1})	Linearity range (mol L^{-1})	Correlation coefficient (r)	Plate number	Separation resolution (R_s)
FITC	0.25	5.0×10^{-7} to 5.0×10^{-3}	0.999	26582	–
SF	0.1	2.5×10^{-7} to 5.0×10^{-3}	0.998	18691	–
D-PA	1.1	6.25×10^{-6} to 1.25×10^{-3}	0.998	16572	1.84

minimum detectable concentration and mass for SF and FITC were 0.25 μmol L^{-1}, 0.09 fM and 0.5 μmol L^{-1}, 0.18 fM, respectively, at 0.37 nL sample injection volume. It seemed that the presented detectable concentration was slightly higher than previous result [10], which was mainly ascribed to the varied chip microchannel size and thickness used in both experiments. Although the results were not compared directly with the commercial fluorometer or traditional LED-IF detection, the present system had demonstrated its advantages such as simple design, low-cost, compact, integration and miniaturization, which may direct the trend for LED-IF detection in microsystem.

In this work, a typical electropherogram of SF was shown in Fig. 5(A). The results exhibited good repeatability with RSD 1.3% and 2.8% for peak height and migration time, respectively. In addition, SF of 625 nmol L^{-1} was detectable for measurement of limit of detection (Fig. 5(B)).

3.4. Application in D/L-penicillamine (PA) separation

To show the potential applicability of this proposed instrumental setup, a practical effort for PA enantiomer separation was carried out. D-PA is therapeutic, and has long been used to treat hepatolenticular degeneration (Wilson's disease) [34]. Whereas the L-enantiomer was highly toxic attributed to the similar configuration as L-amino acids and therefore grossly influenced the amino acid endosomatic metabolism [35]. Thus, a simple, rapid and sensitive analytical method was required to separate and determine the PA enantiomers. To the best of our knowledge, little, if any, studies had been made on the utilization of integrated microfluidic device for PA analysis. Therefore, the present microdevice was employed due to its high separation efficiency, minimum sample requirement and high sensitivity.

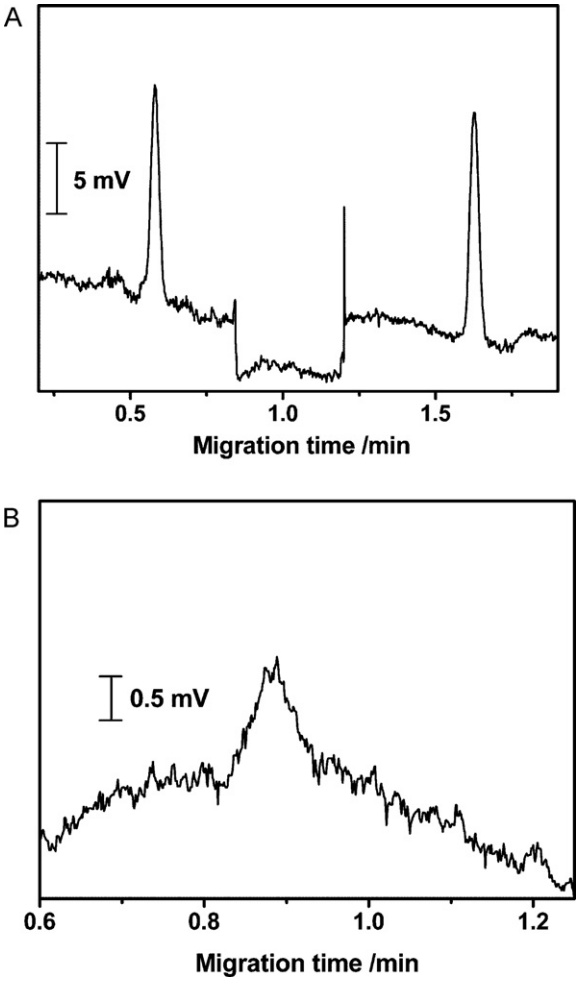

Fig. 5. The electrophorogram of samples. Sample: (A) 20 μmol L^{-1} sodium fluorescence; (B) 625 nmol L^{-1} sodium fluorescence. Operation conditions: electrical current of LED 220 mA; focusing pinhole diameter 1.1 mm; fluorescence collection angle 45°; detection distance 9 mm; injection for 10 s at 0.5 kV; separation voltage, 2.0 kV; running buffer, 10 mmol L^{-1} $Na_2B_4O_7$, pH 9.2.

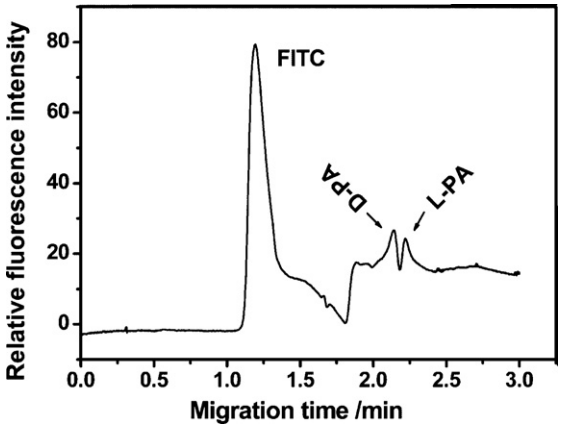

Fig. 6. Electrophoretic separation of D/L-penicillamine mixture derivatized with FITC. Concentration of each enantiomer in the mixture was 25 μmol L^{-1}. Running buffer: 50 mmol L^{-1} $Na_2B_4O_7$, 30 mmol L^{-1} SDS, 7.5 mmol L^{-1} β-CD, pH 9.5; separation channel, 10 cm; other conditions are the same as in Fig. 5.

In this work, we investigated the effect of pH and concentration of the buffer, additive and chiral selector as well as applied voltage on PA enantiomers separation. The pH ranging from 8.0 to 10.0 were studied, and the results demonstrated no obvious improvement for the separation resolution (R_S). But the concentration of buffer, SDS and β-CD had significant influence on R_S, and the optimal condition for a typical electropherogram of PA enantiomer was shown in Fig. 6. Under this experimental condition, the enantiomer realized baseline separation, but the R_S can not be further improved. Presumably, this was because of the relatively large pinhole size, which provided limitations for analytes separation at well resolution, even if the samples had been isolated when a small excitation pinhole employed.

4. Conclusion

In this work, a simplified LED-IF detector has been developed to integrate with a microfluidic system and applied to separate PA enantiomers. Compared to other LED-IF detectors, this set-up consists of only four main elements: a fan-shaped LED, a focusing pinhole, a yellow filter and a flat photodiode, without employing focusing lenses, optical fibers, combined filters and PMT. This design makes the scheme easily home-built, economic, compact and miniaturized. In the study, we use a 1.1 mm diameter focusing pinhole fabricated in a piece of silver foil and a high-power LED with heat sink to improve the sensitivity and make the detector well-suited for more microchip, not limited to the chip with thin cover plate. Moreover, the optical set-up and the electrical circuit system have been compartmentalized into a two-layer analytical device. We have investigated four major influencing factors in detail to optimize the detection sensitivity. Although the current sensitivity is relatively lower than other routine LIF detection, particularly those lasers used as excitation source, it still has potential to be applied in clinical biochemical analysis, like peptides or proteins with high concentration. The sensitivity of this device can further improve with a more compact design and the use of higher power LED and higher responsive photodiodes.

Acknowledgements

Financial supports from National Natural Science Foundation of China (Grant 20727006 and 20875105), and Guangdong Provincial Science and Technology Project (2008A030102009) are gratefully acknowledged.

References

[1] J.L. Fu, Q. Fang, T. Zhang, X.H. Jin, Z.L. Fang, Anal. Chem. 78 (2006) 3827.
[2] W. Qiang, C. Zhai, J.P. Lei, C.J. Song, D.M. Zhang, J. Sheng, H.X. Ju, Analyst 134 (2009) 1834.
[3] J. Lee, S.A. Soper, K.K. Murray, Anal. Chim. Acta 649 (2009) 180.
[4] W. Som-Aum, H. Li, J.J. Liu, J.M. Lin, Analyst 133 (2008) 1169.
[5] S.N. Ding, J.J. Xu, H.Y. Chen, Talanta 70 (2006) 403.
[6] Z.G. Chen, Q.W. Li, O.L. Li, X. Zhou, Y. Lan, Y.F. Wei, J.Y. Mo, Talanta 71 (2007) 1944.
[7] H. Wensink, F. Benito-Lopez, D.C. Hermes, W. Verboom, H. Gardeniers, D.N. Reinhoudt, A. van den Berg, Lab. Chip 5 (2005) 280.
[8] X.J. Yang, Z.G. Chen, C. Liu, O.L. Li, Talanta 82 (2010) 1935.
[9] Z.G. Chen, O.L. Li, C. Liu, X.J. Yang, Sens. Actuators B 141 (2009) 130.
[10] C. Liu, Y.Y. Mo, Z.G. Chen, X. Li, O.L. Li, X. Zhou, Anal. Chim. Acta 621 (2008) 171.
[11] X. Li, Y.L. Tong, C. Liu, O.L. Li, X.J. Yang, Z.G. Chen, Chin. J. Anal. Chem. 37 (2009) 1547.
[12] S. Kim, B. Huang, R.N. Zare, Lab. Chip 7 (2007) 1663.
[13] G.F. Jiang, S. Attiya, G. Ocvirk, W.E. Lee, D.J. Harrison, Biosens. Bioelectron. 14 (2000) 861.
[14] D. Xiao, L. Yan, H.Y. Yuan, S.L. Zhao, X.P. Yang, M. Choi, Electrophoresis 30 (2009) 189.
[15] B. Yao, G. Luo, L.D. Wang, Y.D. Gao, G.T. Lei, K.N. Ren, L.X. Chen, Y.M. Wang, Y. Hu, Y. Qiu, Lab. Chip 5 (2005) 1041.
[16] J.B. Edel, N.P. Beard, O. Hofmann, J.C. DeMello, D. Bradley, A.J. DeMello, Lab. Chip 4 (2004) 136.
[17] O. Hofmann, X.H. Wang, J.C. DeMello, D. Bradley, A.J. DeMello, Lab. Chip 5 (2005) 863.
[18] M.L. Chabinyc, D.T. Chiu, J.C. McDonald, A.D. Stroock, J.F. Christian, A.M. Karger, G.M. Whitesides, Anal. Chem. 73 (2001) 4491.
[19] C.C. Liu, D.F. Cui, X. Chen, J. Chromatogr. A 1170 (2007) 101.
[20] W.B. Du, Q. Fang, Q.H. He, Z.L. Fang, Anal. Chem. 77 (2005) 1330.
[21] A.E. Bruno, F. Maystrea, B. Krattigera, P. Nussbauma, E. Gassmann, Trends. Anal. Chem. 13 (1994) 190.
[22] F.B. Yang, J.Z. Pan, T. Zhang, Q. Fang, Talanta 78 (2009) 1155.
[23] B.C. Yang, F. Tan, Y.F. Guan, Talanta 65 (2005) 1303.
[24] S.L. Zhao, H.Y. Yuan, D. Xiao, Electrophoresis 27 (2006) 461.
[25] O. Hofmann, X.H. Wang, A. Cornwell, S. Beecher, A. Raja, D. Bradley, A.J. DeMello, J.C. DeMello, Lab. Chip 6 (2006) 981.
[26] D.P. Schrum, C.T. Culbertson, S.C. Jacobson, J.M. Ramsey, Anal. Chem. 71 (1999) 4173.
[27] B.C. Yang, Y.F. Guan, Talanta 59 (2003) 509.
[28] Z.H. Liang, N. Chiem, G. Ocvirk, T. Tang, K. Fluri, D.J. Harrison, Anal. Chem. 68 (1996) 1040.
[29] X.F. Yin, S. Hong, Z.L. Fang, Chin. J. Anal. Chem. 31 (2003) 116.
[30] S.T. Li, Q.L. Yu, X. Lu, S.L. Zhao, J. Sep. Sci. 32 (2009) 282.
[31] W.W. Bi, S.R. Lei, X.P. Yang, Z.M. Xu, H.Y. Yuan, D. Xiao, M. Choi, Talanta 78 (2009) 1167.
[32] E.P. de Jong, C.A. Lucy, Anal. Chim. Acta 546 (2005) 37.
[33] L.X. Tan, J. Li, K. Wang, S. Liu, IEEE T. Electron. Pack. 32 (2009) 233.
[34] S. Sinha, A.B. Taly, J. Neurol. Sci. 264 (2008) 129.
[35] N. Mestdagh, J. Poupaert, J.P. Hénichart, J. Vamecq, Biochem. Pharmacol. 43 (1992) 1529.